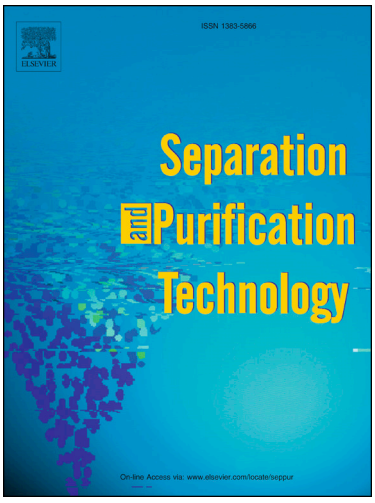

Electrochemical softening of concentrates from an Electrodialysis brackish water desalination plant: efficiency enhancement using a three-dimensional cathode.

Ignacio Sanjuán, David Benavente, Vicente García-García, Eduardo Expósito, Vicente Montiel

PII: S1383-5866(17)33772-3
DOI: https://doi.org/10.1016/j.seppur.2018.01.066
Reference: SEPPUR 14360

To appear in: *Separation and Purification Technology*

Received Date: 17 November 2017
Revised Date: 22 January 2018
Accepted Date: 30 January 2018

Please cite this article as: I. Sanjuán, D. Benavente, V. García-García, E. Expósito, V. Montiel, Electrochemical softening of concentrates from an Electrodialysis brackish water desalination plant: efficiency enhancement using a three-dimensional cathode., *Separation and Purification Technology* (2018), doi: https://doi.org/10.1016/j.seppur.2018.01.066

Electrochemical softening of concentrates from an Electrodialysis brackish water desalination plant: efficiency enhancement using a three-dimensional cathode.

Ignacio Sanjuán[a], David Benavente[b], Vicente García-García[a], Eduardo Expósito[a], Vicente Montiel[a,*]

[a] *Grupo de Electroquímica Aplicada, Instituto Universitario de Electroquímica, Departamento de Química Física, Universidad de Alicante, Apdo. 99, Alicante 03080, Spain.*

[b] *Departamento de Ciencias de la Tierra y del Medio Ambiente, Universidad de Alicante, San Vicente del Raspeig, Alicante 03690, Spain.*

Submitted to: Special issue "Advanced Electrochemical Technologies for Environmental Applications" in Separation & Purification Technology

* Corresponding author:

e-mail addres: vicente.montiel@ua.es (V. Montiel)

Tel.: + 34 965903628

Fax: + 34 965903537

Abstract

The electrochemical softening method to remove hardness from water has not been applied in desalination practice due to a high cathodic area requirement. In this work, the use of a 3D stainless steel wool cathode is proposed to overcome this technical limitation. An extensive comparison between the 3D cathode and a 2D Ti mesh has been presented, showing higher hardness removal for the 3D one. Experiments have been conducted with waters similar to concentrates derived from a brackish water treatment by electrodialysis. In addition, the method has been proved to be efficient for different water compositions in terms of hardness, alkalinity or the presence of an anti-scalant. The main influencing parameters (flow rate and current density) have been studied and it can be concluded that lower flow rates (below 1.2 L h^{-1}) give rise to a better efficiencies and 100 A m^{-2} is the optimum current density. Moreover, the precipitate was characterised by SEM, EDX and XRD showing that Ca^{2+} is removed as calcite and aragonite ($CaCO_3$), whereas Mg^{2+} is precipitated as brucite ($Mg(OH)_2$). Finally, long-term experiments revealed that the 3D stainless steel cathode has a better performance than the 2D Ti mesh, but only at short times.

Keywords: Electrochemical softening, hardness removal, three-dimensional electrodes, electroprecipitation, concentrate, wastewater treatment.

Nomenclature

List of symbols

2D	Two-dimensional
3D	Three-dimensional
A	Ampere
C	Hardness Conversion
DSA	Dimensionally stable electrodes
EC	Specific energy consumption
ED	Electrodialysis
EDX	Energy Dispersive X-Ray Spectroscopy
FO	Forward osmosis
H_o	Initial hardness of the feed water
H_f	Steady state value of final hardness
HMP	Sodium hexametaphosphate
I	Current intensity
ICP-OES	Inductively coupled plasma optical emission spectroscopy
j	Current density
$m_{deposited}$	Mass of the removed insoluble compounds
Q	Flow rate
SEM	Scanning electron microscopy
SSW	Stainless steel wool
t	Time of experiment
V	Volt
V_{cell}	Cell voltage
VMD	Vacuum membrane distillation
XRD	X-ray diffraction

1. Introduction.

The availability of affordable clean water is currently one of the key technological, social, and economic challenges for the scientific community [1]. Most countries of the Mediterranean and Middle East areas suffer a high water stress index. Moreover, there are countries with a positive water balance in spite of the water distribution is not homogeneous, presenting a serious lack of water in some areas [2]. In these regions, precipitations are insufficient to meet the water demand and it makes necessary to resort to underground resources. However, most of these resources have been currently overexploited and some of them suffer from saline contamination [3–5].

Electrodialysis (ED) is a technique based on the transport of ions through selective membranes under the influence of an electric field. This technique has proved its feasibility and high performance in the desalination of brackish water [6–9]. It could be a strategic solution for the problems mentioned above. Nevertheless, one problem limiting the application of this technology is the generation of a concentrate which reduces the amount of recovered water. Besides, this concentrate must be properly managed, increasing both the economic and the environmental costs associated with the treatment [10,11]. It is clearly of great interest to augment the water recovery reducing the volume of concentrate since would make the ED technology more cost-effective. Unfortunately, concentrates coming from the electrodialysis of certain types of brackish water usually present a high amount of scale forming ions such as calcium (Ca^{2+}), magnesium (Mg^{2+}), sulphate (SO_4^{2-}) and hydrogen carbonate (HCO_3^-). In this sense, a reduction of the concentrate volume, with the consequent concentration of solutes, could give rise to a precipitation of insoluble salts leading to scaling problems in installations (pipe plugging, membrane fouling, etc.). Therefore, an adequate scale control measurement should be incorporated after the ED in order to finally recover more water from the concentrate [10,12]. Once the hardness level has been controlled, the concentrate may be treated again by the ED with a corresponding higher water recovery. The advantages of removing hardness from the concentrate rather than directly from the brackish water are the smaller volume and the higher level of hardness. Both facts facilitate the corresponding hardness removal treatment. Several methods are commonly employed with this aim: lowering water pH [13], inducing precipitation by a chemical process [14], blocking crystallization by chemical inhibitors [15] and ion exchange resins [12,16,17]. The main drawbacks of these methods are the

need to add chemical compounds, the increase of the final solution electrical conductivity and the management of wastes. At present, the most employed method is the addition of chemical inhibitors which can prevent the process by adsorption on the crystallization surface [10,18]. Nevertheless, that process involves chemicals which can foul the membranes and are harmful to the human health in drinking water [19].

An interesting alternative method may be the electrochemical precipitation technique [17,19–21]. This method is based on the water electrolysis as described in figure 1. In the cathode, the electroreduction of water takes place to generate hydrogen gas (H_2) and hydroxyl ions (OH^-). Accordingly, the local pH at the cathode vicinity increases causing the deposition of Ca and Mg insoluble compounds on its surface. On the other hand, the reaction on the anode is the water electrooxidation with the generation of oxygen gas (O_2) and hydrogen ions (proton, H^+). The electrochemical way to remove hardness presents several advantages which are mainly [22]: does not require a tedious maintenance, environmental compatibility, avoids any chemicals addition, the possibility of automation and convenient process control. Additionally the insoluble compounds could be recovered and valorised.

Regarding the equipment used, the electrolysers geometry are typically cylindrical with coaxial electrodes or parallelepiped with parallel plates [17]. Cathodes are normally made of non-corrodible materials (stainless steel, titanium, titanium clad iridium, etc.) being stainless steel the most commonly employed. The works presented in literature usually present two-dimensional (2D) plate electrodes of stainless steel. The insoluble layer formed falls down spontaneously or forcibly and is collected at the bottom of the reactor. In the case of the anode, oxygen evolution electrodes are commonly employed. They are made by modification of the surface covering of conventional dimensionally stable electrodes (DSA). They are highly selective electrodes, able to suppress chlorine (Cl_2) generation and promote oxygen (O_2) generation [23].

To date, despite the commercial availability of such equipment, the electrochemical softening technique has been limited only to cooling towers [20]. It has not been applied in the desalination practice due to some technical limitations. One of them is the high electrode area requirement because the deposit adheres to the cathode producing an increase in electrical resistance and thus in the economic cost [12]. Another consists of the existence of a limiting current density (j) beyond which the precipitation rate remains unchanged [24,25]. Thus, the application of this technique for

scale control in the desalination practice needs a major system development in order to reduce the electrode area requirement and provide lower energy consumption.

In the present paper, the electrochemical softening method has been evaluated for hardness removal in water similar to ED concentrates coming from ground waters. A three-dimensional (3D) stainless steel wool (SSW) has been used as cathode in order to enhance the efficiency of the process and to reduce the energy consumption. SSW, also known as wire wool or wire sponge, consists of bundles of fine stainless steel filaments. It is commonly used as an abrasive in finishing and repair work for polishing wood or metal objects, cleaning household cookware, cleaning windows and sanding surfaces. The use of this kind of material as electrode has already been reported by Lopez et al. (2016) [26], where steel wool is employed as 3D anode for electrocoagulation. Other kind of three-dimensional electrodes could be considered like the carbon-based ones. However, the inner spaces of these electrodes structure are smaller than in the case of the aforementioned wool and this could lead to obtain higher pressure drops when the solid is being formed, with the consequent block of the system. Therefore the stainless steel wool was the first choice for this work. We suggest the use of 3D cathodes instead of the common 2D plates. The goal is to provide a more available surface for the scale deposition and therefore to overcome the aforementioned problems which limit the practical application of this technique. Accordingly, an extensive comparison between the 2D and 3D electrodes behaviour is shown. For that, we carried out experiments at the laboratory scale to control the main influencing parameters. Also, we demonstrated the hardness removal efficiency of the system in the presence of an anti-scalant compound. Besides, for a better understanding of the process, the precipitate composition and morphology were characterised. Finally, the efficiency of the system was evaluated with time in long-term experiments for both types of electrode, which is essential to be assessed for a future practical application. The interest of the study lies, as mentioned above, in the development of a more efficient electrochemical system which could allow the practical application of hardness removal in concentrates from the ED of brackish water, increasing the amount of recovered water and diminishing the economic cost of the ED treatment.

2. Materials and methods

2.1. Chemicals and solutions.

Magnesium sulphate heptahydrate ($MgSO_4 \cdot 7H_2O$), calcium chloride dihydrate ($CaCl_2 \cdot 2H_2O$), calcium nitrate tetrahydrate ($Ca(NO_3)_2 \cdot 4H_2O$), sodium bicarbonate ($NaHCO_3$), sodium chloride (NaCl), sodium sulphate anhydrous (Na_2SO_4), sodium hexametaphosphate (HMP, $(NaPO_3)_6$) and ethylenediaminetetraacetic acid disodium salt dihydrate ($Na_2EDTA \cdot 2H_2O$) were purchased from Fluka at the ACS reagent grade (≥99%) and used without any further purification. Sulfuric acid (H_2SO_4) and hydrochloric acid (HCl) reagents were purchased from Sigma-Aldrich (95-97% and 35%, respectively). Ammonium chloride (NH_4Cl) was supplied by VWR Chemicals (99%) and ammonia solution (35%) by Fluka at the analytical reagent grade. Eriochrome Black T indicator (pure, indicator grade) was obtained from Across Organics. Solutions employed in this work were always prepared with deionised water (3 MΩ cm).

2.2. Standard solution composition.

The composition of the feed water pretends to be similar to typical concentrates from brackish water treated by ED (Table 2). For that, a brackish water average concentration was obtained from typical values of underground resources located at the aquifer system Medium Turia (South East of Spain) [27]. Next, the composition of a concentrate was estimated as this brackish water would have been treated by ED. Working solutions (feed water) were freshly prepared before each experiment with a final hardness of 2300 - 2400 ppm as $CaCO_3$ and alkalinity of 1400 – 1500 ppm as $CaCO_3$, unless otherwise stated. Firstly, $MgSO_4 \cdot 7H_2O$, $CaCl_2 \cdot 2H_2O$ and $Ca(NO_3)_2 \cdot 4H_2O$ are mixed in water up to their complete dissolution. Then, small amounts of $NaHCO_3$ were slowly added under vigorous stirring to hinder the nucleation of the insoluble compounds. pH was adjusted to 7.4 (from about 7.8) with a 3% HCl solution, giving rise to an approximately final 1500-1600 ppm of Cl^-. Finally, the solution is filtered (filter paper, ALBET, 7-11 μm pore diameter) in order to remove any formed precipitate. We made sure that, after this procedure, spontaneous nucleation of insoluble compounds in the liquid phase is slow since no significant hardness decrease was observed after 12 hours. The experiments were conducted at room temperature and the temperature of the solutions did not vary significantly during the experiments (temperature always within the range 25 – 28 ^oC).

2.3. Electrolytic system.

System always worked at continuous flow mode and allowed flow rates (Q) in the range of 0.2 L h^{-1} – 2.7 L h^{-1}. All the experiments were performed in the galvanostatic mode, with current densities (j) in the range of 25 – 200 A m^{-2}. The solution is circulated by an ISMATEC REGLO digital peristaltic pump. The power supply employed was a Laboratory Power Supply Elektro Automatik MODEL EA-PS 2032–050 DC. Figure ESI-1 shows a scheme of the experimental system.

Furthermore, Figure 2 displays the scheme of the electrochemical reactor with both employed configurations and a detailed view of its elements. The system was a 100 cm^2 commercial filter-press electrochemical reactor (ElectroMP-Cell, ElectroCell). In this work, we have performed experiments with both the 2D electrode and the 3D one. In both cases, the anode always was a 10 cm x 10 cm oxygen evolution DSA plate (a IrO_2 film onto a Ti plate) in order to minimise the Cl_2 generation.

In the case of the system with a 2D electrode, the used electrode was a Titanium (Ti) mesh of 10 cm x 10 cm of area. The interelectrode gap was 0.8 cm. The electric resistance associated was estimated to be around 2 Ω. This configuration corresponds to the Figure 2A.

For the experiments with a 3D electrode, the Ti mesh employed in the 2D configuration acted as current collector and a 3D SSW (AISI 434) was incorporated as cathode. The target was to achieve an improvement in the process incorporating a 3D electrode to the 2D configuration. Since the process of interest is the water electrolysis, there will not be significant differences between employing Ti and stainless steel as cathodic material because the electrocatalytic activity for the water electroreduction of both materials is similar. 3D electrodes allow the solution to circulate through its structure and two possible configurations are available: the flow-by configuration (current perpendicular to the fluid flow, figure 2A) and the flow-through configuration (current parallel to the fluid flow, figure 2B). Both configurations were tested in this work for the SSW. The piece of wool employed always weighed around 6 g with the following dimensions: 10 cm height x 10 cm length x 1.25 cm width. The geometric cathode area (cross section) of 10 cm x 10 cm was taken into account as active area for the j calculation. The actual area of the SSW cannot be determined easily but it can be estimated to be of 225 cm^2 taking into account the density, the weight and the wire thickness of the wool. The wool wire thickness was within the range 0.06-0.08 mm. It was placed within the hollow of a plastic flow frame and contacting with the current

collector and with a polyethylene mesh. As a result, the piece of wool was contained in a compartment of the following dimensions: 10 cm length x 10 cm height x 0.8 cm thickness. The polyethylene mesh role was to press the cathode against the current collector in order to minimise IR drops and avoid the contact between anode and cathode. The mesh dimensions were 10 cm length x 10 cm height x 0.2 cm thickness and the mesh size was 0.3 cm. The interelectrode gap was 0.3 cm and the associated electric resistance was about 0.75 Ω in this case.

2.4. Standard values for the influencing parameters.

The efficiency of the electrochemical softening technique to remove hardness was tested using the system described in section 2.3. The most influencing parameters were studied in order to understand the process and to know the operational conditions leading to the best efficiency. Standard values for these parameters were previously chosen (Table 1) as reference and it will be stated when some is modified. These values are used as reference when the corresponding parameter is not being studied. In order to determine the standard values of both flow rate and current density we firstly consulted the commonly used working ranges of these parameters in literature [19,24] and we selected the most adequate for the system to use. Afterwards, we performed a row of tests for each parameter to find a specific value which gave rise to a proper result. Regarding the standard values of composition, their choice is explained in section 2.2. SSWs with different wire thickness were evaluated previously but no significant differences were found between them (not shown).

2.5. Instruments and analytical procedures.

Ca^{2+} and Mg^{2+} content in solution was controlled by measuring the total hardness as mg L^{-1} of $CaCO_3$, with the EDTA titrations method [28]. Total alkalinity was measured as well as $CaCO_3$ by a H_2SO_4 potentiometric titration to the end point of pH 4.3 [28]. In both cases an automatic titrator 702 SM Titrino (Metrohm) was used. During the long-term experiments, Ca^{2+} and Mg^{2+} were measured separately by inductively coupled plasma optical emission spectroscopy (ICP-OES, Perkin Elmer, Optima 7400DV, dual vision). pH measurements were carried out by a Crison Micro pH 2000 pH-meter and the electric conductivity was measured by a 4510 JENWAY conductivity meter. Samples were always filtered with a 0.45 μm pore nylon filter

before the analysis. Each sample was measured twice at least in order to check the accuracy of the determination.

The phase composition of precipitates was analyzed by powder X-ray diffraction (XRD) on a Bruker D8-Advance diffractometer with mirror Goebel (non-planar samples) using the Cu Kα radiation and a setting of 40 kV and 40 mA. Data were collected and interpreted using the XPowder software package. The qualitative search-matching procedure was based on the ICDD-PDF2 database. Calcite, aragonite and brucite were identified and quantified by the JCPDS (Joint Committee on Diffraction Pattern) standards 5-0586, 7-1475 and 7-0239, respectively. No other phases were found in the precipitates.

Precipitate morphology and chemical composition of the scale layer on the cathode was carried out under scanning electron microscopy (SEM, HITACHI S-3000N microscope working at 20 kV with X-ray detector Bruker Xflash 3001 for microanalysis). Composition and element distribution (mapping) were performed on uncoated scale layer surfaces. For a better image resolution, samples were coated with a thin gold film produced with an SCD 04 high vacuum evaporator for the morphological observations.

2.6. Performance data.

The effectiveness of the technique was evaluated according to the following parameters: the specific energy consumption (EC, kWh kg^{-1} $CaCO_3$) and the Hardness Conversion (C, %). Therefore, for every experiment, the water hardness is determined after and before its pass through the reactor and the cell voltage (V_{cell}) is measured at all time. Additionally, other parameters are also monitored: the cathode potential vs. AgCl/Ag (3.5 M KCl) standard reference electrode (CRISON), pH, conductivity and temperature. Experiments were carried out at least twice to ascertain the reproducibility of the results. The R is given by:

$$\boldsymbol{C} = \frac{\boldsymbol{H_o - H_f}}{\boldsymbol{H_o}} \cdot \mathbf{100} \qquad (\mathbf{1})$$

where H_o is the initial hardness of the feed water and H_f is the steady state value of final hardness after the experiment, both expressed in mg L^{-1} of $CaCO_3$. Moreover, the EC is given by:

$$EC = \frac{V_{cell} \cdot I \cdot t}{m_{deposited}} \cdot 10^{-3} \quad (2)$$

where V_{cell} is the average cell voltage measured in volts, I is the current intensity in amperes (constant value for each experiment), t is the time of the experiment in hours and $m_{deposited}$ is referred to the removed mass of insoluble compounds, expressed as kg of $CaCO_3$.

3. Results and discussion.

3.1. Effect of the experimental conditions.

3.1.1. Cell configuration.

Two possible cell configurations (Flow-by and Flow-through) are possible when a 3D electrode is employed, as commented in section 2.3. It is interesting to compare both configurations before the experimental performance and determine what is the most adequate. That comparison was made for the 3D SSW and the results are summarised in Table 3. As can be seen, the efficiency in hardness removal is higher in the case of the flow-through configuration while the average V_{cell} is almost the same. As a result, the EC is lower for the flow-through configuration and thus is the chosen for all the experiments.

The better performance of the flow-through configuration could be attributed to a lower accessibility of the HCO_3^- for being consumed by the H^+ generated on the anode. On the one hand, flow-by configuration implies the solution crosses the cathode longitudinally (figure 2A). From a hydrodynamic point of view, the plastic mesh set between the electrodes should favour that the solution circulates preferentially through the area close to the anode rather than through inner spaces of the SSW. In accordance, it is logical to assume that the facility to reach the HCO_3^- will be comparable for both the OH^- and the H^+.

On the other hand, with the flow-through configuration, the solution crosses the entire cathode transversely (figure 2B), from the side opposite to the anode to the other one. In this way, the entire solution comes in contact initially with the cathode but remote from the anode, and circulates necessarily through the inner spaces of the wool. According to this, we can suggest that in this case the OH^- can reach the HCO_3^- more easily than the H^+. As a conclusion, the overall amount of H^+ finally reacting with the HCO_3^- is higher for the flow-by configuration, resulting in a higher alkalinity loss and a

lower efficiency. The final pH of the treated water resulted to be acid in both cases. This is expectable since the precipitation process implies a consumption of OH^- (figure 1). After the electroprecipitation experiments, the treated water conductivity hardly varies respect to the initial feed water (about 4 mS in both cases).

3.1.2. Effect of the flow rate.

Q marks the residence time of the solution in the electrochemical reactor and is consequently a major parameter. In this section, Q in the range 0.5 – 2.5 L h^{-1} were studied for both the 2D and 3D cathodes to compare the hardness removal efficiency and to assess the optimum value of operation. Figure 3 shows the R variation at the steady state with Q for both types of electrodes, together with the pH of the treated water.

In both cases R decreases as the Q increases. It can be also observed that the pH is lower as Q decreases, indicating a better efficiency for low Q. That behaviour is logical because at high Q the feed water passes too fast through the electrochemical reactor leading to an insufficient treatment [17,29]. That means a lower applied charge per cubic meter (Coulombs m^{-3}) and therefore a lower OH^- concentration at every instant. In addition, when water circulates faster, there is a higher stirring of the solution. This fact has important implications since affects the diffusion of ions (reactants and products) between the reaction zone and the solution bulk. In this regard, higher Q promotes the OH^- and H^+ diffusion towards the solution bulk and thus also their neutralisation. In addition, the promoted diffusion of both OH^- and generated CO_3^{2-} towards the solution bulk also contributes to hinder the electroprecipitation since all the reactants have to reach each other necessarily on the cathode vicinity.

Experiments with the 3D SSW achieve better R (about 20-25 percent points higher) and V_{cell} around 1.2 V lower. This can be explained by the interelectrode distance which is lower in the case of the 3D configuration (lower IR drop). The better performance of the 3D configuration vs. the 2D one could follow a similar explanation that in the case of the previous section. As already commented, the 3D cathode with the flow-through configuration implies that the solution crosses the cathode transversely

and through the inner spaces of the wool. In this way, the solution comes in contact initially with the cathode from the side opposite to the anode. It provides lower accessibility of the HCO_3^- for being consumed by the H^+ generated on the anode. In the case of the 2D electrode, the solution circulates longitudinally between the two electrodes and thus the facility to reach the HCO_3^- will be comparable for both the OH^- and the H^+. It should be remarked that precipitation only occurs onto the cathode surface in both cases and is not found in solution because of the low pH.

These results are supported by the final pH, which becomes acidic in the case of the 3D electrode while is maintained almost neutral for the 2D Ti mesh. A lower pH means a higher precipitation since more OH^- have reacted with the HCO_3^- (figure 1). For the 2D electrode, this pH drop at lower flow rates is no observed since the hardness efficiency removal is not high enough. The lowest value of Q 0.5 L h^{-1} presents the highest R although 1.2 L h^{-1} was chosen for the rest of experiments because has good efficiency and, since a practical point of view, it allows to treat more amount of water and gives rise to a pH less acid.

3.1.3. Effect of the current density.

j is known to be one of the most influencing parameters in electrochemical processes to treat wastewater since it has an important effect in the efficiency and high influence on the economic cost. Experiments with j in the range 25 - 200 A m^{-2} were conducted for both 2D and 3D cathodes. Figure 4 depicts the change of R with the j employed. In both cases, it is found that R augments as j increases.

For the 3D electrode R augments up to a certain limit, around 100 A m^{-2}. From this value upwards, part of the electrical energy is consumed to no purpose. The process must be limited by the diffusion kinetics of the reactants towards the reaction zone [19]. Otherwise, for the 2D one this increase is not very pronounced and R does not seem to reach an asymptotic level in the range of j studied. With this electrode the process may not be efficient enough to consume the reactants and reach a mass transfer limit.

R is also higher for the 3D electrode in this case, as figure 4 shows. Since the same amount of OH^- is generated for both electrodes with each j, this better performance must be explained in terms of the commented in the previous section. This can be corroborated by the acidic pH with the 3D electrode compared to the neutral obtained in all the experiments for the 2D one. A higher electrode surface also makes

the generation of H_2 bubbles more dispersed and therefore minimise their stirring effect on the solution. In this regard, the consequent OH^- and CO_3^{2-} diffusion is more difficult, giving rise to a better process efficiency.

Nevertheless, there is a clear exception at the lowest j where the 2D Ti mesh presents a higher R than the 3D SSW. This phenomenon might be explained based on the high active area of the 3D SSW. For the plot of figure 4, the geometric area of 100 cm^2 has been taken into account for the calculation of j. However, the actual active area is considerably higher because of the three-dimensional structure and the actual j obtained in these conditions should be too low to generate sufficient OH^- concentration to remove hardness efficiently.

Table 4 shows the V_{cell} values and the EC calculated for the experiments of figure 4. As expected, it can be observed that for the 3D electrode the EC is about a 65 % lower respect to the 2D one. That supports the better performance of this electrode. It should be taken into account that the interelectrode gap is lower for the 3D electrode system that for the 2D one.

It can be concluded that, once again, the 3D electrode displays a better performance and the j of 100 A m^{-2} is the optimum for this electrode, since higher j hardly improve the results.

3.2. Effect of the solution composition.

After the main operational parameters were investigated in section 3.1., the next step in the study was to evaluate the effect of the solution composition. The purpose was to check the system efficiency for different kinds of water. In this sense, the components tested were those intervening in the electroprecipitation process, that is, the Ca and Mg content (hardness) and the HCO_3^- concentration (alkalinity).

3.2.1. Effect of HCO_3^- concentration.

In the $CaCO_3$ electroprecipitation process, the OH^- generated in the cathode react with HCO_3^- to give rise to an increase of carbonate (CO_3^{2-}) and thus to a phase supersaturation effect (figure 1). In addition, HCO_3^- is an amphoteric ion which presents a pH buffer capacity. According to this, HCO_3^- concentration is a relevant parameter to consider and therefore experiments with different initial HCO_3^- concentration (in the range of 0 - 5500 mg L^{-1} of HCO_3^-) were carried out. In figure 5, the plot R vs. HCO_3^-

concentration can be seen. As figure highlights, R increases when HCO_3^- concentration does for both 2D and 3D electrode. These results also corroborate that the 3D electrode gives better efficiency than the 2D electrode, except for the highest HCO_3^- concentration.

However, R is found to reach a maximum for the 3D electrode at around 1100 mg L^{-1} of HCO_3^-, beyond which the R starts to fall down again. The removal efficiency is thus the highest when the HCO_3^- concentration is close to the equimolarity respect to the hardness level as $CaCO_3$ (the case of the water employed in previous sections). Higher and lower HCO_3^-/hardness ratios give rise to worse efficiencies. A HCO_3^- excess buffers the pH environment avoiding the $Mg(OH)_2$ precipitation. It has been proved by the SEM and XRD analysis of the resultant precipitates since when the feed water presents high alkalinity no evidences of brucite are found. In addition, a high HCO_3^- concentration may not improve the hardness removal due to a limitation in the diffusion kinetics of Ca^{2+} towards the reaction zone. Moreover, a lack of HCO_3^- means no reactant enough for the reaction. On the contrary, for the 2D electrode there is not limit in the range of HCO_3^- concentrations studied. The local pH on the cathode vicinity for the 2D Ti mesh is higher than the one for the 3D SSW and therefore the buffer capacity of the HCO_3^- is not strong enough to avoid the precipitation of $Mg(OH)_2$. As the efficiency is lower for the 2D electrode, no limitation in the Ca^{2+} diffusion kinetics is reached.

It is worth noting that when there is not any amount of HCO_3^- in the feed water, only $Mg(OH)_2$ and no $CaCO_3$ is deposited on the 3D SSW electrode, as determined by SEM and XRD. Interestingly, $Mg(OH)_2$ does not precipitate in the 2D electrode due to OH^- can reach the H^+ more easily than in the 3D configuration because of the explained in the 3.1.2. section.

3.2.2. Effect of hardness degree.

The electrochemical precipitation of Ca and Mg compounds is limited by diffusion of the reactants towards the cathode surface. The previous sections dealt with water of high hardness degree (2300-2400 ppm of $CaCO_3$). In this sense, it is interesting to investigate the influence of hardness degree on the hardness removal efficiency. A series of experiments were carried out for solutions with initial hardness degree in the range of 300 - 2380 mg L^{-1} of $CaCO_3$. The HCO_3^-/hardness ratio for all the experiments

was also kept in equimolarity at all cases. There were not significant differences between the experiments (figure ESI-2) and thus it can be concluded that this system is able to work with waters of different hardness degree without any effectiveness loss. In this case, the 3D experiments also achieved better results than the 2D ones.

3.2.3. Effect of the addition of a precipitation inhibitor compound.

The effectivity of the system to remove hardness in water was also assessed with the presence of an inhibitor compound of the precipitation process: the sodium hexametaphosphate (HMP). HMP is widely used as dispersant agent upon solid materials, such as clays [30]. It is also commonly used as scale inhibitor by the membrane industry since concentrations below 5 mg/L prevents the formation of calcium carbonate scale [31]. The mechanism of HMP as scale inhibitor is based on its adsorption onto the active sites of the crystal growth. This increases the nucleation time and consequently prevents or delays the scale formation [32].

The goal of these experiments was to evaluate whether the inhibitor capacity of the HMP could affect the electrochemical system efficiency. Electrochemical precipitation experiments were conducted for water with 2350 ppm of hardness with the presence of 0.2 mg L^{-1} of HMP. In this experiment only the 3D SSW cathode was employed. The presence of HMP did not have any effect on the hardness removal efficiency in the employed concentration. Nevertheless, it did alter the morphology of the formed precipitate as we will see later, in the following section.

3.3. Characterisation of the precipitated crystals.

The morphology and the chemical composition of the precipitate have been studied for a deeper understanding of the process. Phase characterisation was conducted for a precipitate obtained on the SSW cathode, in the optimum conditions determined in the previous sections. The texture and morphology of the precipitates on the SSW surface were analysed by SEM (figure 6). As can be seen in the figure, the scale layer is distributed heterogeneously over the wires of the stainless steel wool with a considerable thickness. It can be also observed that some areas of the metal surface are not covered, which reveals that the scale layer grows preferentially onto a previously deposited precipitate rather than onto the metallic surface. In addition, figure 6C reveals the detachment of the precipitate likely due to the effect of the hydrogen gas generated, as described by [17]. Both phenomena are significant since the cathode surface can stay

active for a longer time. Besides, the morphology and size of crystals are very variable, which implies the formation of different phases and/or polymorphs of the same mineral. The layer in direct contact with the stainless steel surface presents a different crystal habit that the crystals deposited in more external layers and three main forms can clearly be distinguished: trigonal shape crystals, shrubs of thin needles (see figure 6A and 6B) and rough-surfaced spherulites (figure 7D).

The composition of the scale was determined by Energy Dispersive X-Ray Spectroscopy (EDX) analysis for powder extracted from the precipitate formed on the cathode. EDX spectra were registered for the area depicted in the SEM micrograph of figure 8A, showing the presence of Ca, Mg, O, and traces of S. The relative atomic contributions of Ca and Mg were respectively 21% and 3% in the clearest areas and 14% and 14% for the darkest ones. EDX mapping (figure 7B) supports this analysis since can easily be seen that Mg compounds are located in the darkest areas (highlighted in purple), Ca compounds in the clearest ones (highlighted in green) and S is not detected.

Precipitates were identified and quantified by XRD. The XRD pattern for the precipitate powder is shown in figure 7C. The phase composition 84 wt.% of calcite ($CaCO_3$), 4 wt.% of aragonite ($CaCO_3$), 7 wt.% of brucite ($Mg(OH_2$). No other phases were found with XRD, as magnesian calcite ($Ca_{1-X}Mg_xCO_3$), portlandite ($Ca(OH)_2$), vaterite ($CaCO_3$) or calcium sulfates phases (gypsum, $CaSO_4 \cdot 2H_2O$, and anhydrite $CaSO_4$). Despite calcium sulfates phases are not detected by XRD, some negligible amount of S is present according to the EDX spectra.

Comparing the SEM and the XRD analyses and according to typical shapes of phases, we can deduce that the trigonal shape crystals can be attributed to the calcite polymorph [33][34], the needles may correspond to the aragonite form [35][36] and the spherulites could be assigned to the formation of brucite [17]. Calcite is the most thermodynamically stable $CaCO_3$ form [37] but the presence of Mg in solution promotes the formation of aragonite [36]. Ca and Mg are separately eliminated in different pure compounds (perfect match between d-spacing of the phases in the XRD pattern and their standards) and heterogeneously distributed, as seen in the EDX analysis.

Results conclude that the electrochemical softening technique is adequate to remove hardness from waters whose composition is similar to concentrates from

brackish water treated by ED. Despite the inhibiting effect of Mg^{2+} on the scaling [24], the electrochemical softening technique is appropriate for waters with high hardness degree and high Ca/Mg ratio. The presence of magnesium in solution promotes that a small part of the $CaCO_3$ crystallises as aragonite. The aragonite form is more porous than calcite and therefore beneficial to achieve lower voltages [36]. A more porous precipitate could also be less adherent, which facilitates the cathode cleaning.

Moreover, the effect of the presence of HMP on the precipitate was also studied. Phase characterisation was conducted for a precipitate obtained on the SSW cathode in the optimum conditions as well. The texture and morphology were analysed by SEM. The presence of HMP in the feed water leads to a total loss of the precipitate morphology (figure ESI-3A) since either trigonal shape crystals or the needles found in Figure 6 are not seen in this case. Instead, a precipitate with no defined crystal form is formed. Large agglomerations are present and randomly distributed. Further investigations should be done to compare the adherence between the precipitates formed with and without the presence of HMP.

Precipitates were also identified and quantified by XRD in this case. The XRD pattern for the precipitate powder (Figure ESI-3B) and there is not any difference in the phases detected respect to the found in the absence of HMP. In the employed concentration, HMP seems to prevent each crystal phase growing with its characteristic morphology but no its formation. Nevertheless, the phase composition was 89 wt.% of calcite, 2 wt.% of aragonite, 5 wt.% of brucite. That indicates that calcite formation is favoured by the presence of HMP. No other phases were found with XRD.

3.4. Electroprecipitation treatment by simulation of a cascade of electrochemical cells.

Electrochemical precipitation performance was evaluated for a treatment through a simulation of three consecutive electrochemical cells. The goal was to test whether a multiple treatment could effectively enhance the results. In order to simulate these conditions, the feed water was treated three times by the same reactor in different experiments. That is, water was treated once in a continuous flow mode and collected at the end of the experiment. Then, this resultant water is circulated and treated again through the same reactor with the same mode and operating conditions. The same procedure was carried out once more, simulating a treatment with three consecutive

electrochemical cells. Water pH and the hardness removal were measured after each treatment. In this experiment, only the 3D SSW cathode was employed. Figure 8 shows the R for the water after the treatment with each cell. As can be seen, the treatment with two consecutive cells reaches a R ten percentual points higher than for the treatment with only a cell. As a consequence, the final water pH is more acid. After the treatment with the third cell, the obtained R is only 4 percentual points higher. In this case, the pH does not vary, as could be expected. According to this trend, we can suppose that a fourth electrochemical cell would not improve the hardness removal and thus we can conclude that the optimum treatment is with two cells since after two electrolysis the pH becomes highly acidic and HCO_3^- is mostly removed as CO_2.

3.5. Long-term experiments.

Long-term experiments with the electrochemical system were performed for both the 2D and 3D electrodes in the optimum conditions determined in the previous sections: Q = 1.2 L h^{-1} and j = 200 A m^{-2}. Those values are maintained constants during all the experiment duration. Experiments were conducted for 130 h for both configurations. The cell voltage was registered at all time.

Figure 9A displays the R and the V_{cell} with time during the experiments. Clearly, 3D electrode reaches higher R than 2D electrode at short times but its efficiency is progressively going down to the point of being lower when the experiment is getting closer to 60 h, finally reaching R values around the 10%. This behaviour can be explained by the precipitate formation which is blocking the path of the water through the inner canals of the 3D structure. The final pH of the solution is acid at very short times but it becomes neutral at reaching the 20 h, which agrees with the behaviour discussed above. In the case of the 2D electrode, the R achieves stable R values of about 20% and remains essentially constant during all the experiment. In this case, pH is neutral and stable during all the experiment. Regarding the V_{cell} (figure 9B), during the 130 h is maintained constant for both electrodes being the values for the 3D electrode lower than for the 2D electrode. All the taken samples were analysed by ICP-OES to measure the Ca^{2+} and Mg^{2+} separately. Both components are always removed from the solution in the same ratio (Ratio mg L^{-1} Ca^{2+}/Mg^{2+} equal to 3) during all the experiment.

It can be seen that the incorporation of the 3D electrode enhances the process but there must be a problem with the hydrodynamic of the system when the electrode is

being blocked. This issue should be amended with the assessment of the reactor design. The filter-press reactor is employed in this work as a proof of concept but it does not seem to be the optimum design for this kind of process. Additionally, for a future application of the technique a protocol for a rapid electrode cleaning should be established in order to renew or replace the blocked electrode when a determined value of time or efficiency is reached.

4. Conclusions.

In this work, 3D electrodes have been demonstrated to enhance the efficiency of the electrochemical softening method. A 3D stainless steel wool cathode showed a hardness removal about 20 percent points higher in all the experiments when compared to a 2D Ti mesh and also provided lower energy consumption. After the study of the main influencing parameters, it can be concluded that efficiency increases as flow rate decreases whereas it augments as currents densities do, up to 100 A m^{-2} when an asymptotic level is reached. In addition, the system has been proved to be efficient for different water compositions. The characterisation of the precipitates with SEM-EDX and XRD showed the presence of calcite, aragonite and brucite. Finally, long-term experiments revealed that the 3D stainless steel cathode has a better performance than the 2D electrode at short times (up to 30 h) but unfortunately it is progressively falling down at longer times. A better design and development of the electrochemical system is needed in order to overcome this problem and to take full benefit of the 3D electrode enhancement.

By the electrochemical softening method the scaling potential of the water is noticeably reduced (hardness and alkalinity) and this opens the possibility to treat ED concentrates from brackish water. Further investigations must be carried out in order to test the viability of this procedure to make the ED process more cost-effective.

Acknowledgements.

I. Sanjuán would like to acknowledge the Ph.D. fellowship granted and the material and human resources provided by the University of Alicante and the company Aguas de Valencia, S.A.

References.

[1] W. a Jury, H. Vaux, The role of science in solving the world's emerging water

problems, Proceedings of the National Academy of Sciences. 102 (2005) 15715–15720. doi:10.1073/pnas.0506467102.

[2] UNESCO, World Water Development Report Volume 4: Managing Water under Uncertainty and Risk, 2012. doi:10.1608/FRJ-3.1.2.

[3] J.C. Cerón, A. Pulido-Bosch, Geochemistry of thermomineral waters in the overexploited Alto Guadalentin aquifer (south-east Spain), Water Research. 33 (1999) 295–300. doi:10.1016/S0043-1354(98)00175-4.

[4] P. Pulido-Leboeuf, Seawater intrusion and associated processes in a small coastal complex aquifer (Castell de Ferro, Spain), Applied Geochemistry. 19 (2004) 1517–1527. doi:10.1016/j.apgeochem.2004.02.004.

[5] J.M. Ortiz, E. Expósito, F. Gallud, V. García-García, V. Montiel, V. a. Aldaz, Desalination of underground brackish waters using an electrodialysis system powered directly by photovoltaic energy, Solar Energy Materials and Solar Cells. 92 (2008) 1677–1688. doi:10.1016/j.solmat.2008.07.020.

[6] N. Kabay, M. Demircioglu, E. Ersöz, I. Kurucaovali, Removal of calcium and magnesium hardness of electrodialysis, Desalination. 149 (2002) 343–349. doi:10.1016/S0011-9164(02)00807-X.

[7] J.M. Ortiz, E. Expósito, F. Gallud, V. García-García, V. Montiel, A. Aldaz, Electrodialysis of brackish water powered by photovoltaic energy without batteries: direct connection behaviour, Desalination. 208 (2007) 89–100. doi:10.1016/j.desal.2006.05.026.

[8] G. Amy, N. Ghaffour, Z. Li, L. Francis, R.V. Linares, T. Missimer, et al., Membrane-based seawater desalination: Present and future prospects, Desalination. 401 (2016) 16–21. doi:10.1016/j.desal.2016.10.002.

[9] V.G. Gude, Desalination and sustainability - An appraisal and current perspective, Water Research. 89 (2016) 87–106. doi:10.1016/j.watres.2015.11.012.

[10] N. Afrasiabi, E. Shahbazali, RO brine treatment and disposal methods, Desalination and Water Treatment. 35 (2011) 39–53. doi:10.5004/dwt.2011.3128.

[11] AFFA, Introduction to desalination technologies in Australia, 2002. http://scholar.google.com/scholar?hl=en&btnG=Search&q=intitle:Introduction+to+Desalination+Technologies+in+Australia#0.

[12] D. Hasson, G. Sidorenko, R. Semiat, Calcium carbonate hardness removal by a novel electrochemical seeds system, Desalination. 263 (2010) 285–289. doi:10.1016/j.desal.2010.06.036.

[13] H. a. Becker, J.J. Cohen, A.D. Zdunek, Electrochemical cooling water treatment: a new strategy for control of hardness, scale, sludge and reducing water usage, ASHRAE Transactions. 115 PART 1 (2009) 399–404.

[14] N.V. Malanova, V.V. Korobochkin, V.I. Kosintsev, The Application of Ammonium Hydroxide and Sodium Hydroxide for Reagent Softening of Water, Procedia Chemistry. 10 (2014) 162–167. doi:10.1016/j.proche.2014.10.028.

[15] V.B. Obraztsov, E.D. Rubl'ova, O.S. Baskevych, Influence of the Scaling Inhibitor on the Phase Composition, Morphology, and Sedimentation Properties of CaCO3 Deposits, Materials Science. 51 (2016) 652–658. doi:10.1007/s11003-

016-9887-3.

[16] J.N. Apell, T.H. Boyer, Combined ion exchange treatment for removal of dissolved organic matter and hardness, Water Research. 44 (2010) 2419–2430. doi:10.1016/j.watres.2010.01.004.

[17] C. Gabrielli, G. Maurin, H. Francy-Chausson, P. Thery, T.T.M. Tran, M. Tlili, Electrochemical water softening: principle and application, Desalination. 201 (2006) 150–163.

[18] X. Li, H. Shemer, D. Hasson, R. Semiat, Characterization of the effectiveness of anti-scalants in suppressing scale deposition on a heated surface, Desalination. 397 (2016) 38–42. doi:10.1016/j.desal.2016.06.022.

[19] K. Zeppenfeld, Electrochemical removal of calcium and magnesium ions from aqueous solutions, Desalination. 277 (2011) 99–105. doi:10.1016/j.desal.2011.04.005.

[20] D. Hasson, H. Shemer, R. Semiat, Removal of scale-forming ions by a novel cation- exchange electrochemical system — A review, Desalination and Water Treatment. (2015) 1–15.

[21] S.L. Zhi, K.Q. Zhang, Hardness removal by a novel electrochemical method, Desalination. 381 (2016) 8–14. doi:10.1016/j.desal.2015.12.002.

[22] K. Rajeshwar, J.G. Ibanez, G.M. Swain, Electrochemistry and the environment, Journal of Applied Electrochemistry. 24 (1994) 1077–1091.

[23] I. Zaslavschi, H. Shemer, D. Hasson, R. Semiat, Electrochemical CaCO3 scale removal with a bipolar membrane system, Journal of Membrane Science. 445 (2013) 88–95. doi:10.1016/j.memsci.2013.05.042.

[24] D. Hasson, G. Sidorenko, R. Semiat, Low electrode area electrochemical scale removal system, Desalination and Water Treatment. 31 (2011) 35–41. http://www.tandfonline.com/doi/abs/10.5004/dwt.2011.2389.

[25] D. Hasson, V. Lumelsky, G. Greenberg, Y. Pinhas, R. Semiat, Development of the electrochemical scale removal technique for desalination applications, Desalination. 230 (2008) 329–342. doi:10.1016/j.desal.2008.01.004.

[26] A. López, D. Valero, L. García-Cruz, A. Saez, V. García-García, E. Expósito, et al., Characterization of a new cartridge type electrocoagulation reactor (CTECR) using a three-dimensional steel wool anode, Journal of Electroanalytical Chemistry. In press (2016). doi:10.1016/j.jelechem.2016.10.036.

[27] Instituto Geológico y Minero de España, Las aguas subterráneas en la Comunidad Valenciana. Uso, calidad y perspectivas de utilización., IGME, 1988.

[28] E.W. Rice, R.B. Baird, A.D. Eaton, L.S. Clesceri, Standard Methods for the Examination of Water and Wastewater, American Public Health Association; American Water Works Association; Water Environment Federation, 2012. doi:ISBN 9780875532356.

[29] S. Zhi, S. Zhang, A novel combined electrochemical system for hardness removal, Desalination. 349 (2014) 68–72. doi:10.1016/j.desal.2014.06.023.

[30] M. Ma, The dispersive effect of sodium hexametaphosphate on kaolinite in saline water, Clays and Clay Minerals. 60 (2012) 405–410. doi:10.1346/CCMN.2012.0600406.

[31] D. Hasson, A. Cornel, Effect of residence time on the degree of CaCO3 precipitation in the presence of an anti-scalant, Desalination. 401 (2017) 64–67. doi:10.1016/j.desal.2016.06.006.

[32] D.E. Abd-El-Khalek, B.A. Abd-El-Nabey, Evaluation of sodium hexametaphosphate as scale and corrosion inhibitor in cooling water using electrochemical techniques, Desalination. 311 (2013) 227–233. doi:10.1016/j.desal.2012.11.017.

[33] M. Dinamani, P.V. Kamath, R. Seshadri, Electrochemical synthesis of calcium carbonate coatings on stainless steel substrates, Materials Research Bulletin. 37 (2002) 661–669.

[34] J. Rinat, E. Korin, L. Soifer, A. Bettelheim, Electrocrystallization of calcium carbonate on carbon-based electrodes, Journal of Electroanalytical Chemistry. 575 (2005) 195–202. doi:10.1016/j.jelechem.2004.09.011.

[35] C. Gabrielli, G. Maurin, G. Poindessous, R. Rosset, Nucleation and growth of calcium carbonate by an electrochemical scaling process, Journal of Crystal Growth. 200 (1999) 236–250. doi:10.1016/S0022-0248(98)01261-5.

[36] R. Jaouhari, A. Benbachir, A. Guenbour, C. Gabrielli, J. Garcia-Jareno, G. Maurin, Influence of Water Composition and Substrate on Electrochemical Scaling, Journal of The Electrochemical Society. 147 (2000) 2151–2161. doi:10.1149/1.1393501.

[37] J.Y. Gal, Y. Fovet, N. Gache, Mechanisms of scale formation and carbon dioxide partial pressure influence. Part I. Elaboration of an experimental method and a scaling model, Water Research. 36 (2002) 755–763. doi:10.1016/S0043-1354(01)00270-6.

Figures

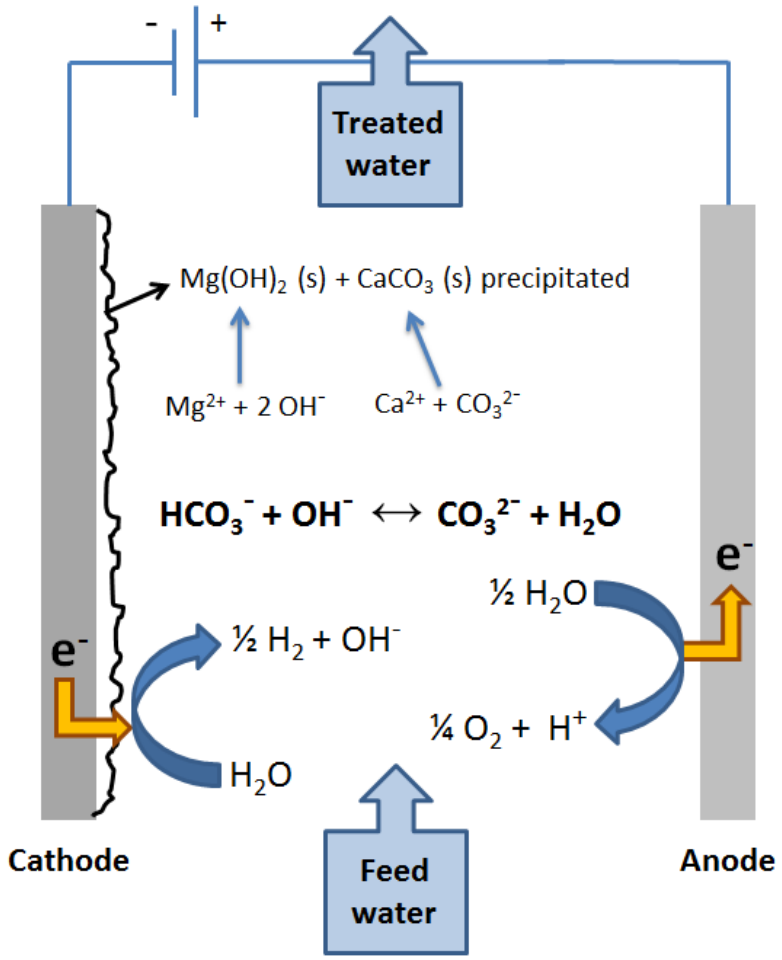

Fig. 1. Scheme of the electrochemical softening process.

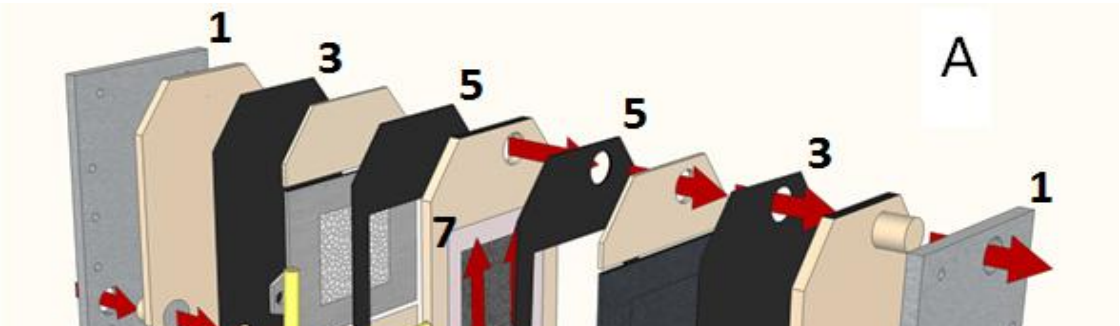

Fig. 2. Schemes of the filter press reactor. A) For the 3D SSW flow-by configuration and the 2D Ti mesh. 1 - End plates. 2 — Plastic end frame. 3 — Rubber sealing. 4 — Ti mesh (current collector) between two spacers. 5 — Rubber sealing. 6 — Flow frame set. 7 — *For the Ti mesh experiments* - Plastic turbulence promoter. *For the 3D SSW flow-by experiments* - Stainless steel wool cathode 8 — DSA-O_2 anode between two spacers. 9 — Reference electrode. B) For the 3D SSW flow-through configuration. 1 - End plates. 2 — Plastic end frame. 3 — Rubber sealing. 4 — Flow frame set. 5 — Rubber sealing. 6 — Ti mesh (current collector) between two spacers. 7 — Stainless steel wool cathode set in the inner space of a flow frame set. 8 — DSA-O_2 anode. 9 —Reference electrode. The passage of the feed water through the reactor is followed by the red arrows.

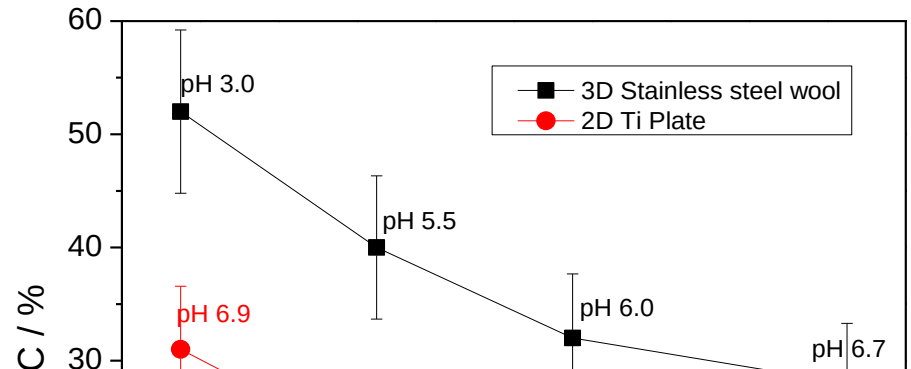

Fig. 3. Plot of hardness conversion vs. flow rate, for both 2D (red circles) and 3D electrodes (blacks squares). pH values for the treated water of each experiment are indicated above its corresponding point. Experiments were performed in the flow-through configuration.

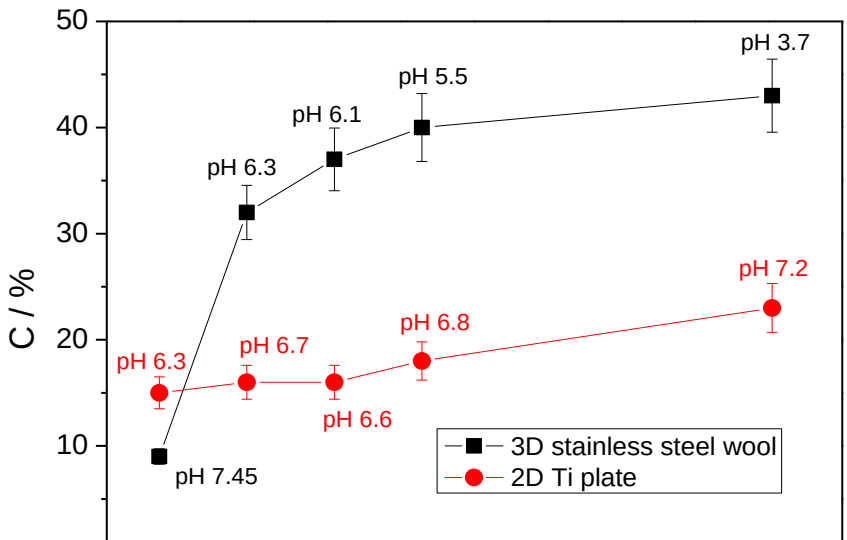

Fig. 4. Plot of hardness conversion vs. current density, for both 2D (Red circles) and 3D electrodes (Black squares). pH values for the resultant water in each experiment are set above its corresponding point. Experiments were performed in the flow-through configuration.

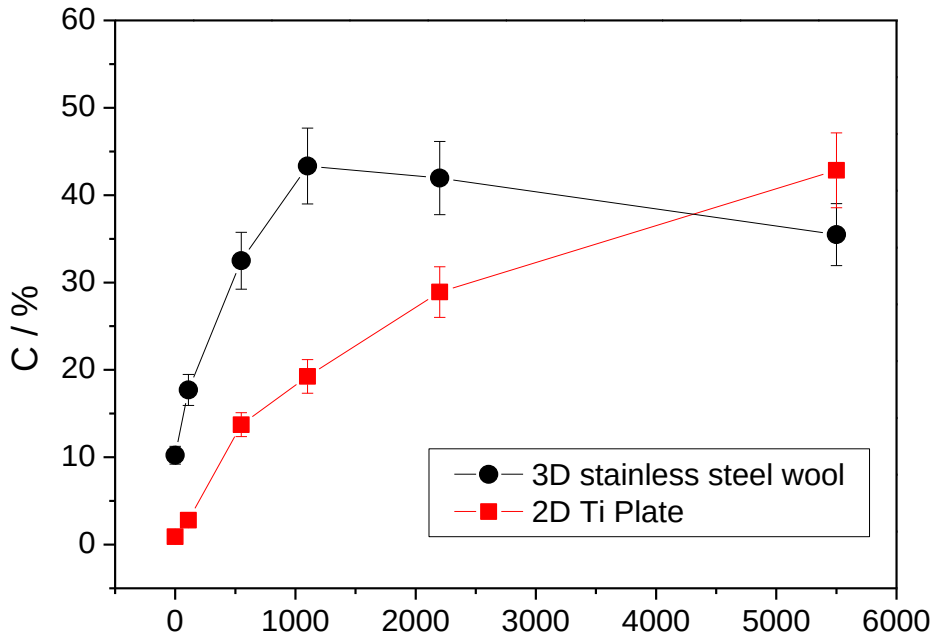

Fig. 5. Hardness conversion vs. HCO_3^- initial concentration, for both 2D (Red squares) and 3D electrodes (Black Circles). (Q = 1.2 L h^{-1}, j = 100 A m^{-2}). Experiments were performed in the flow-through configuration.

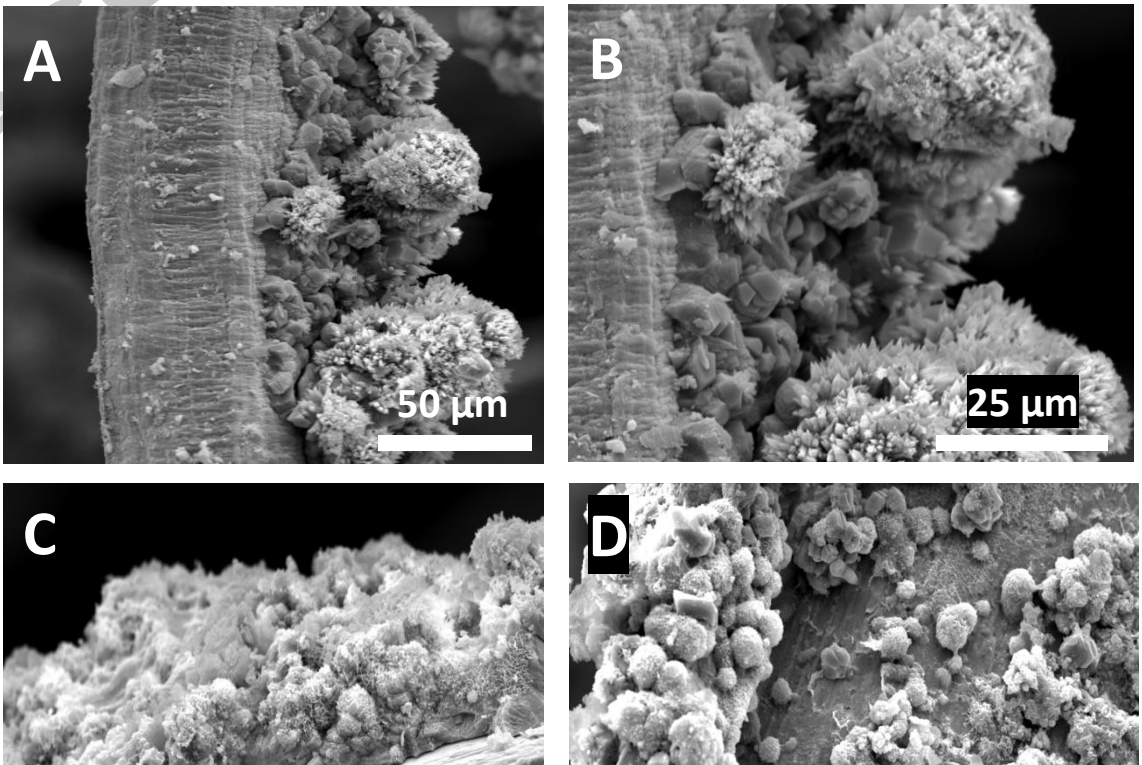

Fig. 6. SEM micrographs of the stainless steel wool cathode with a deposited precipitate. Each micrograph is corresponded to a different area except for A and B which correspond to the same area but different zoom.

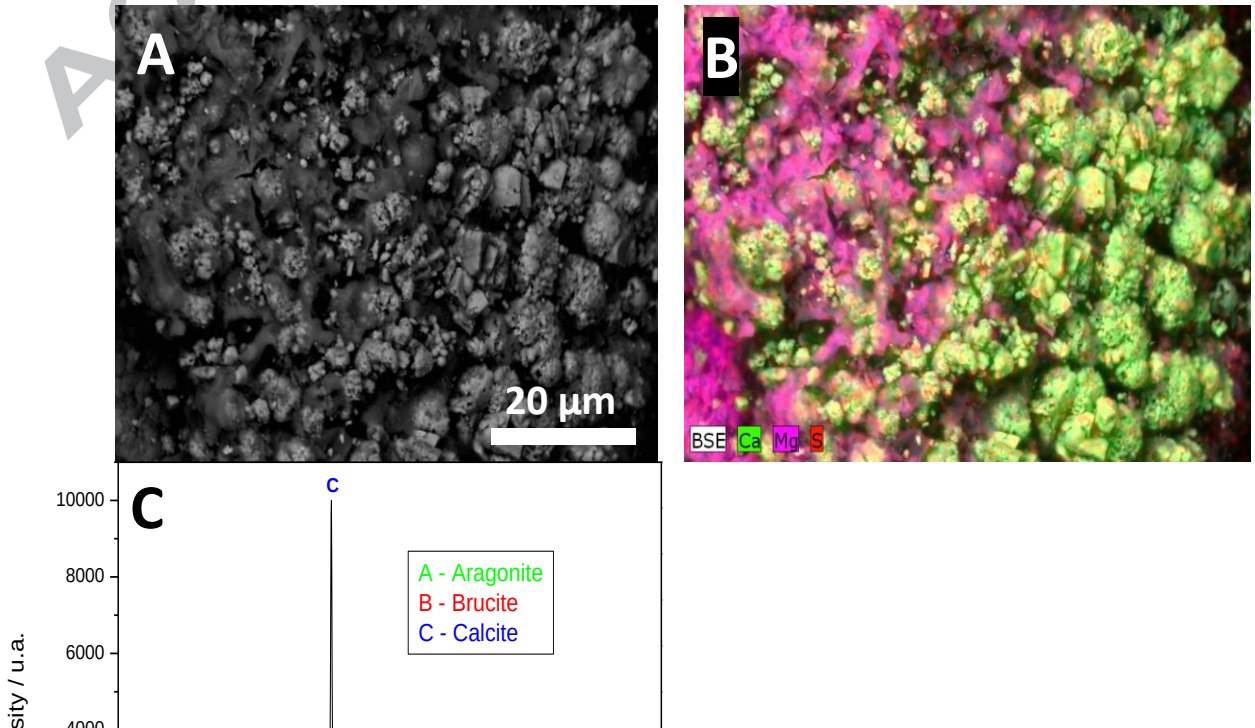

Fig. 7. A) SEM micrograph of the powder extracted from the precipitate on the cathode. B) Mapping image highlights in colours the distribution of Ca (green), Mg (purple) and S (red) in the sample of micrograph A, as detected by EDX. C) Powder XRD diffractogram registered. Each peak is assigned to its corresponding mineral form (A - Aragonite, B - Brucite, C - calcite).

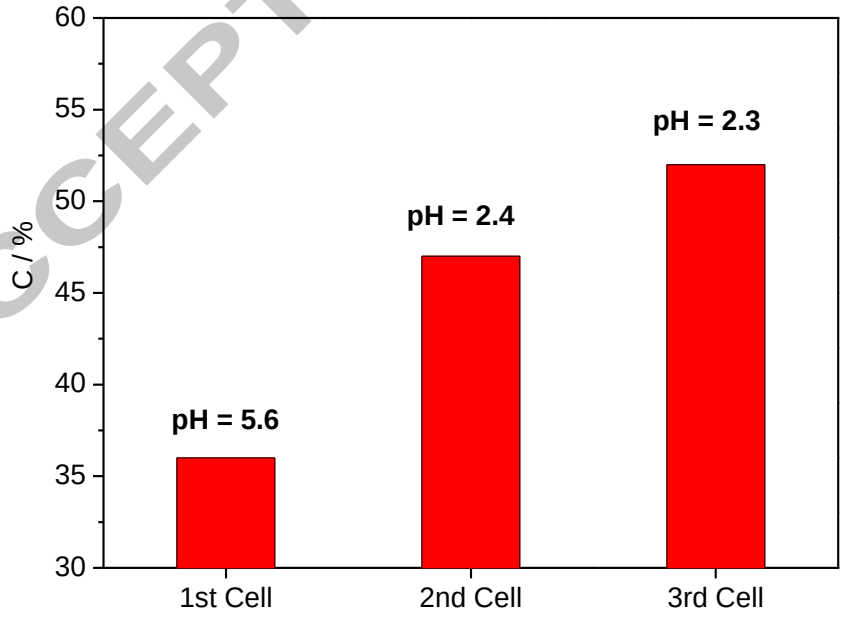

Fig. 8. Plot of hardness conversion for the treated water during a treatment with three consecutive electrochemical cells. The C value is measured after the pass of the water through

each cell, in the steady-state. The experiment has been conducted for the 3D SSW cathode. pH values for the resultant water are set above its corresponding point. Experiments were performed in the flow-through configuration.

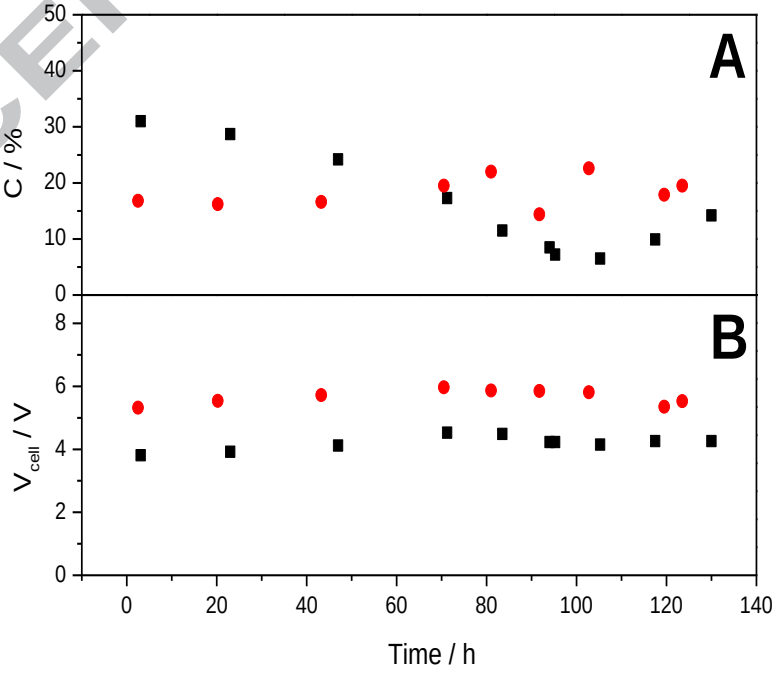

Fig. 9. Plot of A) hardness conversion vs. the time and B) cell voltage vs. time, for both 2D (Red circles) and 3D electrodes (Black squares). Experiments were performed in the flow-through configuration.

TABLES

Table 1: standard values for the most influencing parameters (j, Q).

Parameter	j / A m^{-2}	Q / L h^{-1}	Hardness / mg L^{-1} $CaCO_3$	Alkalinity / mg L^{-1} $CaCO_3$
Value	100	1.2	2350	1400

Table 2: standard chemical composition of the synthetic feed water.

Component	Mg^{2+}	SO_4^{2-}	Ca^{2+}	Cl^-	NO_3^-	Na^+	HCO_3^-

Concentration / mg L^{-1}	200	770	600	1000	800	400	850

Table 3: Experimental data obtained for hardness removal experiments with both the flow-by and the flow-through configurations. Experiments were carried out with the 3D stainless steel wool cathode.

Configuration	**V_{cell} / V**	**Outlet pH**	**R / %**	**EC / kWh kg^{-1} $CaCO_3$**

Flow-through	3.90	5.5	35 - 45	3.2
Flow-by	3.96	5.7	20 - 25	5.1

Table 4. Cell voltage and specific energy consumption values for the experiments of figure 5. Each value is followed by its corresponding standard deviation obtained from 3 different experiments.

Parameter	j / A m^{-2}	2D electrode	3D electrode
Voltage / V	25	3.3 ± 0.2	1.85 ± 0.19
	50	4.03 ± 0.13	2.78 ± 0.05
	75	4.70 ± 0.05	3.2 ± 0.2
	100	5.38 ± 0.09	3.4 ± 0.4

	200	7.57± 0.15	3.9 ± 0.2
EC / kWh kg^{-1} $CaCO_3$	25	6.7 ± 0.4	7.9 ± 0.8
	50	7.8 ± 0.2	3.4 ± 0.8
	75	9.09 ± 0.10	3.3 ± 0.2
	100	9.33 ± 0.16	3.3 ± 0.4
	200	10.8 ± 0.2	3.49 ± 0.18

Highlights

- 3D cathodes provide an enhancement in the electrochemical softening method.
- A comparison between a 2D and a 3D cathode is reported for water hardness removal.
- Long-term electroprecipitation experiments assess the 3D cathode behaviour with time.
- Water hardness is removed by precipitation of calcite, aragonite, and brucite.

Graphical Abstract